Int J Earth Sci (Geol Rundsch) (2017) 106:2359–2369
DOI 10.1007/s00531-016-1431-z

ORIGINAL PAPER

Bismuth selenides from St. Andreasberg, Germany: an oxidised five-element style of mineralisation and its relation to post-Variscan vein-type deposits of central Europe

Alexandre Raphael Cabral[1,4] · **Wilfried Ließmann**[1,2] · **Wei Jian**[3] · **Bernd Lehmann**[1]

Received: 20 March 2016 / Accepted: 30 November 2016 / Published online: 30 December 2016

Abstract Carbonate veinlets at Roter Bär, a former underground mine in the polymetallic St. Andreasberg vein district of the Harz Mountains, Germany, host selenide minerals that are characterised as Bi–Ag-bearing clausthalite (PbSe), tiemannite (HgSe), guanajuatite (Bi_2Se_3) and a number of selenides of Bi, Zn, Cu, Ag and Pd. An unnamed Bi–Pb–Ag selenide species with some Hg and Cu, ideally $Bi_4Pb_3Ag_2Se_{10}$, is reported here. Specular hematite is disseminated within the clausthalite, at the marginal zones of which other selenide minerals are located. The occurrence of bohdanowiczite ($AgBiSe_2$) and umangite (Cu_3Se_2) constrains the formation temperature to $\leq$120 °C, and the selenide–hematite assemblage (plus barite in the carbonate gangue) identifies highly oxidised conditions. Selenide assemblages of Pb, Bi, Ag, with and without Co and Ni, occur in many parts of the Variscan basement of central Europe (Harz, Erzgebirge, Schwarzwald and Bohemian Massif) and represent a high-oxidation variety of five-element (Ag–As–Bi–Co–Ni) veins.

Keywords Polymetallic veins · Bismuth · Selenides · St. Andreasberg · Harz Mountains

Introduction

Reduced selenium species have a much broader stability range than reduced sulfur species with respect to oxidation state of aqueous systems, a fundamental condition for the deposition of selenide minerals (Goldschmidt and Hefter 1933; Simon et al. 1997; Xiong 2003). Chalcophile metals in selenide minerals instead of sulfides can thus provide an insight into the conditions of mineral formation. Bismuth is one of such metals, often associated with the metalloids arsenic and antimony. All three elements occur dominantly as hydroxide or hydroxide–chloride complexes in hydrothermal systems and are highly soluble under oxic conditions, but much less soluble under reducing conditions, with the general solubility pattern of As > Sb > Bi. At 100 °C, for example, the hydrothermal solubility of their oxides is on the order of hundreds of ppm for As, tens of ppm for Sb and for Bi on the order of ppm. Solubilities of As_2S_3/AsS/As, Sb_2S_3 and Bi_2S_3 are orders of magnitude lower (Wood et al. 1987; Pokrovsky et al. 1996, 2006; Tooth et al. 2013).

Here, the geochemical behaviour of Bi is addressed by describing a selenide occurrence at Roter Bär, a former underground mine in the polymetallic veins of St. Andreasberg in the Harz Mountains, Germany. In addition to Ag and base-metal sulfides, Roter Bär has selenide-mineral assemblages (Geilmann and Rose 1928; Ließmann and Bock 1993;

✉ Bernd Lehmann
bernd.lehmann@tu-clausthal.de

Alexandre Raphael Cabral
alexandre.cabral@tu-clausthal.de; alexandre.cabral@kit.edu

Wilfried Ließmann
wilfried.liessmann@tu-clausthal.de

Wei Jian
weijian851@gmail.com

[1] Mineral Resources, Technische Universität Clausthal, Adolph-Roemer-Str. 2A, 38678 Clausthal-Zellerfeld, Germany

[2] Lehrbergwerk Grube Roter Bär Sankt Andreasberg, Rosdorfer Weg 33a, 37073 Göttingen, Germany

[3] MLR Key Laboratory of Metallogeny and Mineral Assessment, Institute of Mineral Resources, Chinese Academy of Geological Sciences, Beijing 100037, China

[4] Present Address: Karlsruher Institut für Technologie, Adenauerring 20b, 76131 Karlsruhe, Germany

Cabral et al. 2015). More than mineralogical curiosities, selenide minerals can fingerprint the formation conditions of economically significant metalliferous deposits, such as those of the unconformity-related type. Our local observations are expanded to central Europe, indicating that selenide veins likely represent a high-oxidation variety of sulfide-rich, five-element (Ag–As–Bi–Co–Ni) veins.

Background information on geology and mineralisation

Roter Bär is situated in the St. Andreasberg Ag–Pb–Zn–Cu vein district (Fig. 1), about 1 km south of the Brocken granite in the Harz Mountains, within its contact aureole. The local geology comprises an Early Carboniferous low-grade metamorphic sequence of slate, greywacke and marble, affected by the Variscan orogeny and thermally metamorphosed to hornfels facies (Geilmann and Rose 1928; Ließmann and Bock 1993). The Brocken granite crystallised in the late stage of the Variscan orogeny, at ca. 295 Ma (Schoell 1970; Baumann et al. 1991).

The Palaeozoic metasedimentary sequence of the Harz Mountains formed the Variscan basement to Early Permian red beds, volcanic rocks and evaporites, which are preserved in the Ilfeld and Meisdorf basins, south and north of the Harz Mountains, respectively. These successions were covered by the Zechstein Sea, the first transgression of which deposited the Kupferschiefer. Long-lasting subsidence all over the Central European Basin formed a thick Mesozoic sequence of chemical and siliciclastic sediments. Extensional tectonics controlled large-scale fluid movement

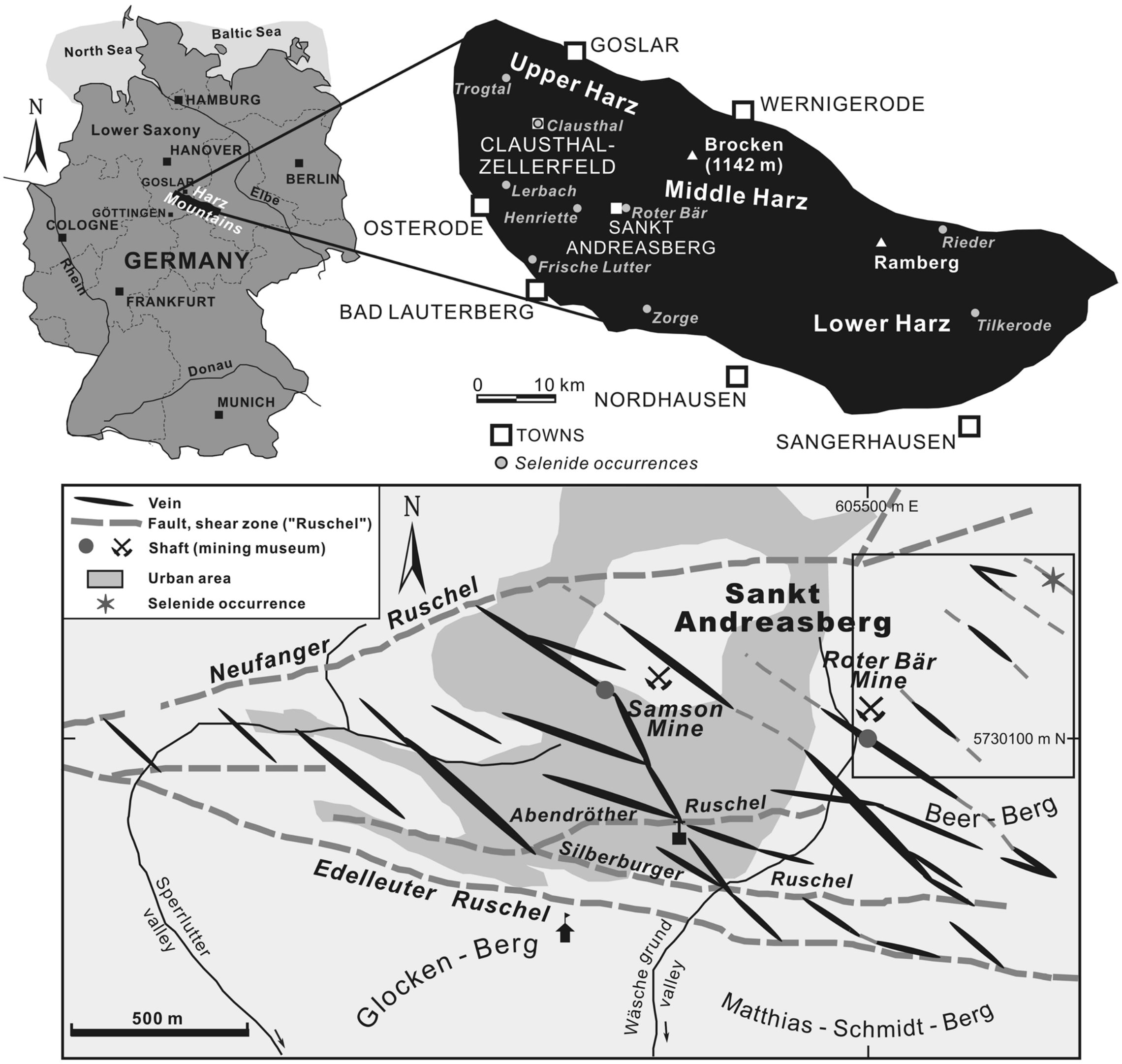

Fig. 1 *Upper* Location of the silver-mining district of St. Andreasberg in the Harz Mountains. *Lower* Sketch of vein distribution at St. Andreasberg and location of the selenide occurrence described here (*asterisk*); *square* indicates the area of underground workings of the Roter Bär mine

of both basinal and basement brines, which formed the Kupferschiefer mineralisation at Sangerhausen, in the Harz piedmont and elsewhere, and also polymetallic vein-style mineralisation in the Variscan basement of the Harz Mountains and elsewhere. The age of these hydrothermal events is bracketed between about 130 and 260 Ma (Mertz et al. 1989; Hagedorn and Lippolt 1993; Boness et al. 1990; Schneider et al. 2003; Symons et al. 2011). The 2–3-km-thick Mesozoic cover strata were eroded from the Harz during rapid Upper Cretaceous basin inversion and exhumation accompanied by reactivation of Variscan and post-Variscan NW–SE- to WNW–ESE-striking fault systems (von Eynatten et al. 2008).

The St. Andreasberg mining district consists of a number of WNW–ESE- and NW–SE-striking quartz–carbonate veins with the typical polymetallic main-phase mineral assemblage of the Harz Mountains: galena, sphalerite, chalcopyrite and tetrahedrite. However, locally, a carbonate phase with elevated silver contents ('Edle Kalkspat-Formation') and the unusual mineral assemblage of native arsenic, antimony, bismuth and silver, plus pyrargyrite–proustite, dyscrasite and various base-metal sulfides/sulfosalts/arsenides, produced irregular bonanza-style silver mineralisation. This peculiar mineralisation style is worldwide known as the 'five-element vein-style mineralisation' (Ag–As–Bi–Co–Ni; Kissin 1992; Markl et al. 2016), which was first observed in the Erzgebirge and there became known as the 'Bi–Co–Ni–Formation' (Oelsner 1958). In the St. Andreasberg district, these silver-rich ore shoots occur over the full mining depth of about 800 m (in the Samson mine, the deepest mine in the district). The total mine production from 1521 to 1910 is estimated at 313 t Ag, 12,500 t Pb and 2500 t Cu (Wilke 1952), but the total silver production from the Harz Mountains is about 5000 t Ag, of which about half came from the main-phase sulfide assemblage in the Bad Grund mine (Stedingk and Stoppel 1993).

At the Roter Bär mine in the easternmost part of the St. Andreasberg mining district, previous microscopic investigation indicated a number of selenide minerals in thin hematite-bearing calcite veinlets, a few centimetres in thickness, hosted in thermally metamorphosed greywacke (Geilmann and Rose 1928). Chemical analysis of the bulk ore (after separation of the carbonate–quartz gangue), in combination with mineralogical work, allowed Geilmann and Rose (1928) to identify the representative ore components as: clausthalite (PbSe) (80 vol%), tiemannite (HgSe) (15 vol%), guanajuatite (Bi_2Se_3) (2.5 vol%), zinc selenide (today: stilleite) (ZnSe) (0.8 vol%), naumannite (Ag_2Se) (0.5 vol%), umangite (Cu_3Se_2) and berzelianite (Cu_2Se) (0.7 vol%), chalcopyrite ($CuFeS_2$) (0.3 vol%), cobaltite (CoAsS) (0.3 vol%), native gold (traces). The presence of umangite is noteworthy because it decomposes above about 110 °C (Chakrabarti and Laughlin 1981). Further investigation led Ließmann and Bock (1993) to recognise adularia and the following selenide minerals: klockmannite (CuSe), bohdanowiczite ($AgBiSe_2$), eucairite (CuAgSe) and ferroselite ($FeSe_2$), as well as an unnamed Bi–Pb–Ag selenide. Recent work on the historical sample material from Rose (1927) identified mertieite-II [$Pd_8(Sb,As)_3$] and empirical $PdCuBiSe_3$ intergrown with clausthalite and gold (Cabral et al. 2015). According to the paragenetic sequence of Wilke (1952), the selenide occurrence belongs to the latest stage of vein mineralisation in the St. Andreasberg district, after the main sulfide mineralisation. However, elsewhere in the Harz Mountains, main-stage sulfide veins are considered to have been preceded by a hematite–carbonate overprint, locally with selenide minerals (Tischendorf 1959; Kuschka and Franzke 1974).

The argentiferous, main-stage sulfide-vein mineralisation of the St. Andreasberg district has been considered genetically related to the Brocken granite (Wilke 1952; Möller et al. 1979). This view, nonetheless, has not been held by some authors (e.g. Tischendorf 1959; Baumann and Werner 1968; Kuschka and Franzke 1974). Dating of vein adularia from St. Andreasberg constrains the end of the main-stage sulfide mineralisation to 136 ± 3 Ma (Ar–Ar age; Mertz et al. 1989), which is younger than the Triassic age ascribed to the sulfide mineralisation at Bad Grund (238 ± 20 Ma, Rb–Sr dating of illite; Boness et al. 1990) and elsewhere in the eastern Harz (226 ± 1 Ma, Rb–Sr dating of illite; Schneider et al. 2003). These ages and a similar broad spectrum of ages for post-Variscan hydrothermal systems in central and western Europe indicate repeated brittle deformation and fluid activity related to large-scale geotectonic processes (Romer et al. 2010).

Sample material and analytical methods

The sample location is in the north-easternmost part of the district (Fig. 1). There, selenide mineralisation was found in 1924 during exploration work carried out by the mining company Ilseder Hütte. An adit, the Neuer Bärener Querschlag, was driven perpendicular to the Wennsglückt vein at 170 m from the entrance of the Sieberstollen adit in the NE direction about 200 m below the surface. The mineralisation comprised three NW–SE-striking carbonate-rich veins (dipping 60°–85°NE) in tourmalinised greywacke hornfels with sericite–quartz–carbonate alteration, at 678, 681 and 700 m NE of the Wennsglückt vein in the Sieberstollen (Geilmann and Rose 1928). These sites are no longer accessible. The sample material investigated here was recovered from a 3–8-cm-thick veinlet located at 678 m (Fig. 2a). The specimen is a 3-cm-thick fragment of ankerite-rich vein. The ankerite-rich vein does not cut the main-stage sulfide-vein mineralisation and no selenide minerals occur in the host rock. Aggregates of ore minerals, here characterised as selenide minerals (see below), form pockets in the host vein carbonate (ankerite and calcite).

Reflected-light microscopy was followed by electron-microprobe work using a Cameca SX 100 instrument at the Technische Universität Clausthal (TUC), Germany. Semi-quantitative analyses were carried out in the energy-dispersive mode to recognise major and minor elements, which were selected for quantitative measurements in the wavelength-dispersive mode. Selenide minerals were analysed at 20 kV and 20 nA, with a beam diameter of 2 µm. Reference materials and X-ray lines were as follows: PbS for S*K*α and Pb*M*α; HgS for Hg*M*α; and pure metals for Bi*M*α, Ag*L*α, Cu*L*α and Se*L*α.

Results

Clausthalite is the main selenide mineral in the ore sample studied, making up a massive matrix in which other minerals are hosted (Fig. 2b). The clausthalite is argentiferous, with Ag contents between 1.1 and 1.3 wt% (Table 1). The mineral also contains Bi in amounts between 2.5 and 3.3 wt% (Table 1). The clausthalite has inclusions of hematite, which manifests itself as subhedral to euhedral, tabular crystals (Figs. 2b, 3a). Yellowish crystals of strong anisotropy are concentrated at marginal zones within the clausthalite matrix (Fig. 3b).

The anisotropic aggregates consist of a Pb–Bi–Ag selenide with some Hg and Cu and, subordinately, a Ag–Bi selenide. They are best distinguished from each other under backscattered-electron imaging (Fig. 4), where the light-grey and dark-grey domains are richer in Bi and Ag, respectively (Fig. 4, X-ray maps). The less abundant Ag–Bi selenide has 21.9 wt% Ag and 42.4 wt% Bi (Table 2), corresponding to bohdanowiczite ($AgBiSe_2$), with some Pb (1.5–3.7 wt%).

The Hg–Cu-bearing Ag–Pb–Bi selenide has 31.2–34.2 wt% Bi, 29.6–30.7 wt% Se, 21.7–26.1 wt% Pb and 6.1–7.9 wt% Ag, with 4.2–5.5 wt% Hg and minor, but noticeable, contents of 0.7–1.0 wt% S and 0.5–0.9 wt% Cu (Table 2). Its average composition is 32.5 wt% Bi, 30.3 wt% Se, 24.1 wt% Pb, 6.8 wt% Ag, 4.8 wt% Hg, 0.8 wt% S, 0.7 wt% Cu, amounting to 100.0 wt% ($n = 16$). Atomic ratios of $\sum$ metal:(Se+S) show narrow variations, between 0.89 and 0.92, with a mean value of 0.91. Using the average chemical composition and 19 atoms per formula unit [*apfu*; to comply with the ratio $\sum$ metal:(Se+S) = 9:10], an empirical formula is obtained:

$$(Bi_{3.79}, Pb_{2.83}, Ag_{1.55}, Hg_{0.59}, Cu_{0.27})_{9.03}$$
$$(Se_{9.36}, S_{0.61})_{9.97} \text{ or, ideally, } Bi_4Pb_3Ag_2Se_{10}.$$

Besides hematite, present as inclusions in the massive clausthalite, some chalcopyrite occurs in contact with, or close to, the surface of the clausthalite. The distribution of

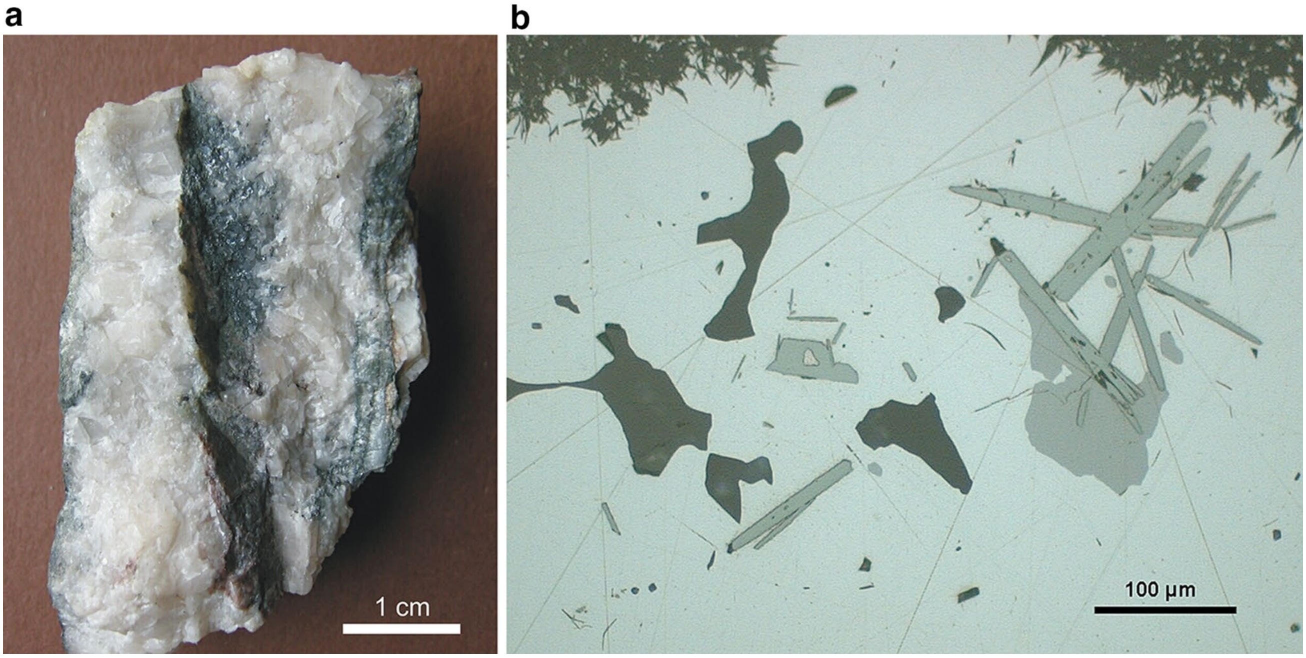

Fig. 2 **a** Photograph of selenide-rich pockets (metallic grey) within a 3-cm-thick ankerite-rich veinlet (*white*). The specimen was sampled at 678 m north of the Wennsglückt vein in the former Roter Bär mine (Geilmann and Rose 1928). **b** Typical mineral assemblage of the veinlet with euhedral, tabular hematite (*medium grey*) and xenomorphic tiemannite (*medium grey*) in clausthalite matrix (*light grey*). Interstitial spaces (*dark grey*) consist of ankerite and calcite. Aggregates of tiny needles (*black*) are probably illite. Reflected light, oil immersion

Table 1 Electron-microprobe analyses of clausthalite from Roter Bär, St. Andreasberg

wt%	1	2	3	4	5	6	7	8	9	10
Ag	1.16	1.31	1.21	1.12	1.21	1.28	1.11	1.05	1.19	1.15
Bi	2.56	3.28	2.69	2.51	2.74	2.68	2.59	2.46	2.45	2.55
Pb	68.53	67.51	68.23	69.21	68.59	68.08	67.92	68.60	68.83	69.09
S	0.33	0.49	0.50	0.42	0.53	0.45	0.31	0.34	0.28	0.42
Se	27.32	27.22	27.20	27.42	26.99	27.24	27.72	27.40	27.52	27.29
Total	99.90	99.81	99.83	100.68	100.06	99.73	99.65	99.85	100.27	100.50
afpu										
Ag	0.030	0.034	0.031	0.029	0.031	0.033	0.029	0.027	0.031	0.030
Bi	0.035	0.044	0.036	0.034	0.037	0.036	0.035	0.033	0.033	0.034
Pb	0.932	0.913	0.923	0.932	0.928	0.923	0.922	0.932	0.933	0.933
Σ metals	1.00	0.99	0.99	0.99	1.00	0.99	0.99	0.99	1.00	1.00
S	0.029	0.043	0.044	0.037	0.046	0.039	0.027	0.030	0.025	0.037
Se	0.975	0.966	0.966	0.969	0.958	0.969	0.987	0.977	0.979	0.967
(Se+S)	1.00	1.01	1.01	1.01	1.00	1.01	1.01	1.01	1.00	1.00

Measurements for Cu and Hg were below the detection limits of 0.4 wt% for both metals

apfu atoms per formula unit

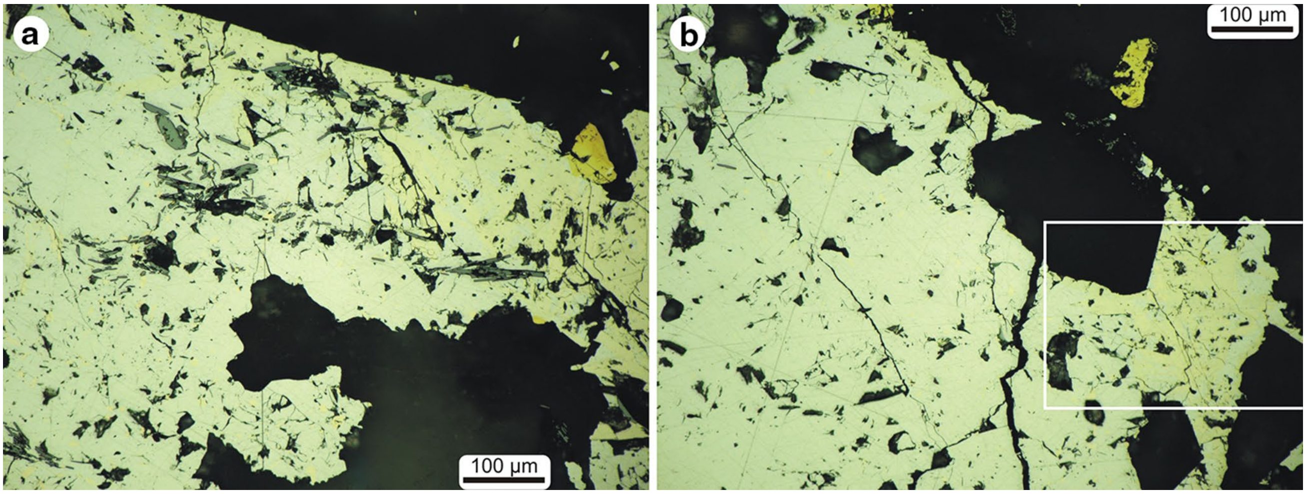

Fig. 3 Reflected-light photomicrographs (oil immersion) of clausthalite (*white*) with inclusions of hematite (*grey*) and gangue (*black*). *Pale-yellowish* selenide minerals occur at the margin of clausthalite. Chalcopyrite (*yellow*) is located on (**a**), or close to (**b**), the surface of the clausthalite aggregate. *Rectangle* delineated in **b** defines the area investigated in Fig. 4

ore minerals suggests a paragenetic sequence from early clausthalite and hematite, followed by bohdanowiczite and the empirical $Bi_4Pb_3Ag_2Se_{10}$ together with clausthalite, to late chalcopyrite that was deposited on top of the hematite–selenide aggregate.

Discussion

The Roter Bär selenide occurrence has a distinctive Bi signature that is expressed as Ag–Bi-bearing clausthalite and a number of Bi-bearing selenides (bohdanowiczite, guanajuatite, empirical $Bi_4Pb_3Ag_2Se_{10}$ and $PdCuBiSe_3$). Clausthalite with about 1 wt% Bi and bohdanowiczite occur at Niederschlema–Alberoda, an unconformity-related vein-type U deposit in the western Erzgebirge, Germany (Förster 2005). Niederschlema–Alberoda contains a variety of Bi selenides (Förster et al. 2005), being the type locality of schlemaite, a Cu–Pb–Bi selenide (Förster et al. 2003). The Bi-selenide mineralogy links Roter Bär not only to Niederschlema–Alberoda, but also to other unconformity-related vein-type deposits in central Europe. A pertinent case is the Zálesí vein-type U deposit in the northern margin of the Bohemian Massif, Czech Republic (Dolníček

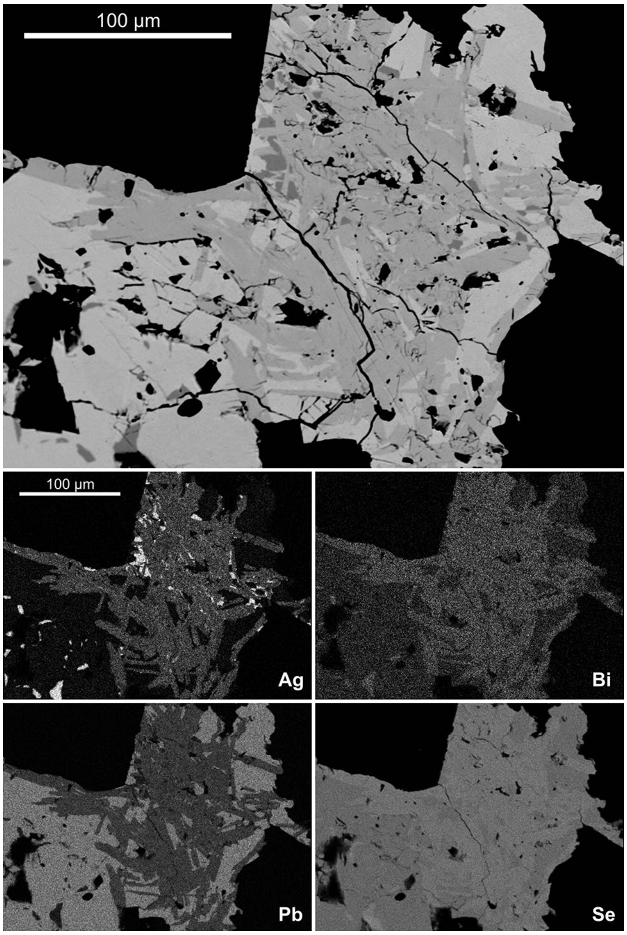

Fig. 4 Backscattered-electron (BSE) image of the area marked in Fig. 3b. The *pale-yellowish* minerals of the latter are now resolved as *dark- and light-grey* phases in the white matrix of clausthalite. X-ray maps show the distribution of Ag, Bi, Pb and Se. The *dark- and light-grey* phases in the BSE image are quantitatively characterised in Table 2 as, respectively, bohdanowiczite ($AgBiSe_2$) and empirical $Bi_4Pb_3Ag_2Se_{10}$

et al. 2009). Zálesí is the type locality of litochlebite (Sejkora et al. 2011), a Bi–Pb–Ag selenide, the composition of which is the one best approaching that of the empirical $Bi_4Pb_3Ag_2Se_{10}$ from Roter Bär. All three deposits, Roter Bär, Niederschlema–Alberoda and Zálesí, have umangite and hematite associated with their Bi-selenide species, indicating high-oxidation conditions at temperatures of up to about 110 °C. We note that umangite has not been observed in our sample material, but it was identified at Roter Bär by Geilmann and Rose (1928). Umangite has commonly been reported from other selenide occurrences of the Harz Mountains (Table 3).

Uranium typically occurs in the five-element vein-style mineralisation—that is, Ag–As–Bi–Co–Ni (Kissin 1992)—which also includes Se. Although the Harz vein systems have little U, it should be noted that uraninite is part of the Roter Bär mineral paragenesis (Wilke 1952), as well as that of Tilkerode in the eastern Harz, where bohdanowiczite and a variety of selenide minerals are found (Table 3; Tischendorf 1959; Stanley et al. 2002; Stedingk et al. 2016). Roter Bär, Tilkerode and other selenide occurrences of the Harz Mountains (Table 3), together with the aforementioned examples in the Erzgebirge and Bohemian Massif, do generally present a spectrum of metals, such as Bi, Ag, Co and Ni, which form sulfide–arsenide associations that are typical of the five-element vein-style mineralisation. Another example of this mineralisation style is the Clara mine, Schwarzwald, the Bi–Se component of which is mineralogically expressed as bohdanowiczite in fluorite veins (Markl 2015).

The Bi–Se component and the ubiquitous hematite, nonetheless, diverge from the classic five-element vein-style mineralisation, which has metallic silver, bismuth and arsenic followed by Co–Ni–Fe arsenides (e.g. Markl et al. 2016). Such a divergence can be explained by different oxidation states: selenide minerals and hematite precipitate at higher fO_2 than those at which metallic silver and bismuth, and arsenides form (Fig. 5; see also Staude et al. 2012). In much of the hematite stability field, ratios of total reduced selenium to total reduced sulfur, $\Sigma H_2Se/\Sigma H_2S$, are >100 (Xiong 2003). Under such conditions, any late sulfide mineral eventually present—as is the case of the late chalcopyrite recorded in the Rote Bär hematite–selenide assemblage—represents exhaustion of ΣH_2Se.

Another divergence arises from mechanisms of metal precipitation. Whereas abrupt changes in redox are thought to play a major role in metal precipitation in five-element veins (e.g. Markl et al. 2016), high Se concentrations in combination with high-oxidation fluids are required to form selenide minerals (Simon et al. 1997). Such differences are reflected in sulfide–arsenide assemblages that are either preceded or followed by selenide assemblages, as encountered in unconformity-related deposits. For example, selenide assemblages followed sulfide–arsenide minerals at Chaméane, in the Massif Central of France (Johan et al. 1982). It may therefore be valid to regard the selenide occurrences of the Harz Mountains as part of the five-element vein spectrum.

Bohdanowiczite as temperature-constraining mineral

Bohdanowiczite has commonly been reported together with umangite (Banaś et al. 1979; Pringle and Thorpe 1980; Förster et al. 2005; Sejkora et al. 2011). Both minerals have stability temperatures that are independent from each other; therefore, textural equilibrium between umangite and bohdanowiczite is not a sine-qua-non requirement for temperature constraining. In the Cu–Se system, the mineral umangite is stable below about 110 °C (Chakrabarti and

Table 2 Electron-microprobe analyses of Ag–Bi selenides from Roter Bär, St. Andreasberg

wt%	1	2	3	4	5	6	7	8	9	10	11	12	13	14	15	16	17	18	19
Ag	22.27	21.51	21.77	6.91	6.25	6.61	6.41	6.45	6.43	6.83	6.99	6.13	7.86	6.97	6.54	7.57	7.68	7.06	6.71
Bi	43.15	42.34	41.78	31.91	32.36	31.75	32.21	32.38	31.34	31.24	33.31	31.24	33.66	32.81	32.53	33.84	34.15	32.07	32.60
Cu	<0.4	<0.4	<0.4	0.62	0.69	0.60	0.54	0.82	0.87	0.75	0.75	0.51	0.61	0.82	0.73	0.92	0.74	0.58	0.80
Hg	0.43	0.45	<0.4	4.58	5.00	4.62	4.83	5.23	4.54	4.87	5.23	5.49	4.23	4.80	4.96	4.73	4.76	4.94	4.65
Pb	1.53	2.00	3.71	24.84	24.19	25.45	24.79	24.32	26.11	25.93	22.60	25.63	22.36	23.59	23.85	21.73	21.87	24.52	23.57
S	0.37	0.22	0.22	0.71	0.95	0.88	0.95	0.78	0.85	0.74	0.84	0.73	0.75	0.85	0.81	0.78	0.68	0.84	0.74
Se	32.58	32.61	32.95	30.44	29.78	29.64	30.20	30.33	30.04	30.29	30.52	29.95	30.69	30.07	30.66	30.68	30.68	30.31	30.50
Total	100.33	99.13	100.43	100.01	99.22	99.55	99.93	100.31	100.18	100.65	100.24	99.68	100.16	99.91	100.08	100.25	100.56	100.32	99.57
afpu																			
Ag	0.975	0.957	0.957	1.567	1.426	1.509	1.451	1.457	1.454	1.541	1.571	1.407	1.765	1.575	1.475	1.692	1.723	1.592	1.521
Bi	0.976	0.972	0.948	3.734	3.811	3.742	3.765	3.777	3.658	3.638	3.864	3.701	3.900	3.826	3.786	3.905	3.954	3.733	3.814
Cu				0.239	0.267	0.233	0.208	0.315	0.334	0.287	0.286	0.199	0.232	0.314	0.279	0.349	0.282	0.222	0.308
Hg	0.010	0.011		0.558	0.613	0.567	0.588	0.635	0.552	0.591	0.632	0.678	0.511	0.583	0.601	0.569	0.574	0.599	0.567
Pb	0.035	0.046	0.085	2.932	2.873	3.026	2.922	2.861	3.074	3.046	2.644	3.062	2.613	2.775	2.800	2.529	2.554	2.879	2.781
Σ metals	2.00	1.99	1.99	9.03	8.99	9.08	8.93	9.04	9.07	9.10	9.00	9.05	9.02	9.07	8.94	9.04	9.09	9.02	8.99
S	0.055	0.033	0.033	0.542	0.729	0.676	0.724	0.593	0.647	0.562	0.635	0.564	0.566	0.646	0.614	0.587	0.513	0.637	0.564
Se	1.949	1.981	1.978	9.428	9.281	9.247	9.342	9.362	9.281	9.336	9.369	9.390	9.412	9.281	9.444	9.370	9.401	9.338	9.445
(Se+S)	2.00	2.01	2.01	9.97	10.01	9.92	10.07	9.96	9.93	9.90	10.00	9.95	9.98	9.93	10.06	9.96	9.91	9.98	10.01

1–3 bohdanowiczite, *4–19* Hg–Cu-bearing Bi–Pb–Ag selenide

apfu atoms per formula unit

Laughlin 1981). In the $AgBiS_2$–$AgBiSe_2$ system, hexagonal $AgBiSe_2$ transforms to a rhombohedral form above 120 °C (Wernick 1960). Since natural $AgBiSe_2$ is the hexagonal mineral bohdanowiczite, the occurrence of bohdanowiczite indicates formation temperatures of ≤120 °C. Such low temperatures are supported by the finding of bohdanowiczite as an authigenic mineral, formed below 100 °C, in the cores of reduction spheroids from Permian red beds of northern Switzerland (Hofmann 1990; vide below discussion on metallogenetic implications).

Bismuth as brine fingerprint

Direct evidence for the involvement of brines at Roter Bär is lacking; no fluid-inclusion studies are available. Nevertheless, the empirical phase $Bi_4Pb_3Ag_2Se_{10}$ contains Pb and Ag,

Table 3 Main characteristics of selenide occurrences of the Harz Mountains

Locality	Host rock (age)	Mineralisation style	Selenide minerals
Clausthal	Greywacke (Early Carboniferous)	Quartz vein	cl, na, tie and Co selenide
Frische Lutter (Bad Lauterberg)	Greywacke (Early Carboniferous)	Quartz–barite vein	boh, cl, gua
Henriette (Sieber)	Greywacke (Early Carboniferous)	Quartz–barite vein	cl, boh, nev, kl, um
Lerbach	Slate and metabasite (Middle Devonian)	Quartz–ankerite vein	be, cl, kl, kr, tie, um and Tl-bearing selenides (cr, sa)
Rieder (Gernrode)	Greywacke (Early Carboniferous)	Ankerite–hematite vein	be, cl, eu, kl, na, tie, um and Co–Ni selenides (tro, ty)
Roter Bär (St. Andreasberg)	Greywacke (Early Carboniferous)	Ankerite vein	be, boh, cl, eu, fe, gua, kl, na, st, tie, um, unnamed minerals $Bi_4Pb_3Ag_2Se_{10}$ (this work) and $PdCuBiSe_3$
Tilkerode	Graptolite shale (Wenlockian) and metabasite	Ankerite–hematite vein	at, be, boh, ch, cl, ge, kl, na, tie, tis, um and Co–Ni selenides (bor, fr, pe, tro, trü, ty)
Trogtal	Greywacke (Early Carboniferous)	Dolomite–hematite vein	cl, eu, fe, tie and Co–Ni selenides (bor, fr, pe, tro)
Zorge	Slate and metabasite (Middle Devonian)	Quartz–ankerite vein	at, be, cl, kl, na, tie, um and Tl-bearing selenides (cr, sa)

Localities are indicated in Fig. 1. Mineral abbreviations: *at* athabascaite, *be* berzelianite, *boh* bohdanowiczite, *bor* bornhardtite, *ch* chrisstanleyite, *cl* clausthalite, *cr* crookesite, *eu* eucairite, *fe* ferroselite, *fr* freboldite, *ge* geffroyite, *gua* guanajuatite, *kl* klockmannite, *kr* krutaite, *na* naumannite, *pe* penroseite, *sa* sabatierite, *st* stilleite, *tie* tiemannite, *tis* tischendorfite, *tro* trogtalite, *trü* trüstedtite, *ty* tyrrellite, *um* umangite

Data source Belendorff (1997), Cabral et al. (2012, 2015), Frebold (1927), Geilmann and Rose (1928), Heider (2014), Heider and Siemroth (2012), Keutsch et al. (2009), Koch (2008), Ließmann and Bock (1993), Ramdohr and Schmitt (1955), Stanley et al. (2002), Stedingk et al. (2016), Tischendorf (1959), Wallis (1994)

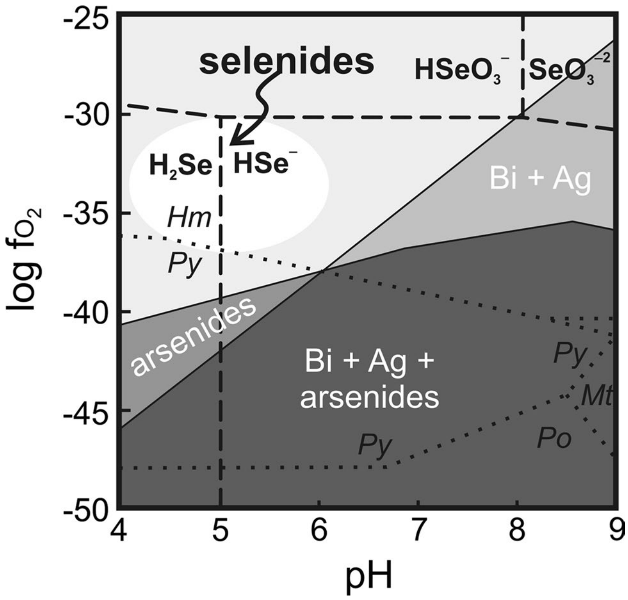

Fig. 5 Diagram of pH versus log fO$_2$ at 200 °C for iron minerals (*dotted lines*) and aqueous selenium species (*dashed lines*)—data from Xiong (2003)—superimposed on the predominance fields of metallic silver and bismuth and arsenides (skutterudite and safflorite), as calculated by Markl et al. (2016). The field where selenide minerals form is schematically depicted (*arrowed*). The Bi–Ag–Se mineral assemblage of Roter Bär can be regarded as an oxidised variant of the five-element vein-style mineralisation. *Hm* hematite, *Mt* magnetite, *Po* pyrrhotite, *Py* pyrite

which are efficiently transported as chloride complexes in a wide spectrum of hydrothermal environments (e.g. Wood et al. 1987; Wood and Samson 1998), particularly in oxidised solutions poor in reduced sulfur, a necessary condition to deposit selenide minerals. Therefore, it is reasonable to propose that empirical $Bi_4Pb_3Ag_2Se_{10}$ was deposited from oxidised brines in which Bi, Pb and Ag were soluble as chloride complexes.

Evidence for high-salinity Na–Ca–Cl brines at relatively low temperatures of 100–180 °C comes from fluid-inclusion microthermometry of minerals from several post-Variscan hydrothermal fluid systems in the Harz Mountains, such as hematite–carbonate veins and main-stage sulfide mineralisation (Lüders and Möller 1992). Further evidence for oxidised brines is available from other occurrences of Bi selenides in post-Variscan veins. In the Erzgebirge, hydrothermal solutions responsible for the polymetallic and U mineralisation, which includes Bi-selenide minerals, were brines trapped at homogenisation temperatures below 200 °C (e.g. Thomas and Tischendorf 1987). At Zálesí, trapped brines have highly variable halogen ratios that indicate derivation from evaporated sea water, possibly from the overlying Permian–Triassic evaporitic sequences (Dolníček et al. 2009). Such a Zechstein-derived origin for fluid salinities found in the post-Variscan vein-type deposits has also been suggested by S-isotope data of sulfide minerals from the Harz Mountains (e.g. Zheng and Hoefs 1993), the Spessart (Wagner et al. 2010) and regional studies in western Europe (Dill 1994; Schmidt Mumm and Wolfgramm 2004), as well as by Cl/Br ratios of fluid inclusions from various post-Variscan vein systems in central and western Europe (e.g. Fusswinkel et al. 2013; Burisch et al. 2016; Walter et al. 2016).

Age of selenide minerals at Roter Bär

According to Wilke (1952), the Roter Bär selenide minerals belong to the latest hydrothermal stage. In contrast, Kuschka and Franzke (1974) consider the hematite-bearing overprint, locally with selenide minerals, as the oldest hydrothermal stage, younger than the Early Permian (Ilfeld basin). A precise age for the hematite–selenide assemblage at Roter Bär remains uncertain. It is pertinent, nonetheless, to note that hematite-impregnated adularia from the Hasserode vein system near Wernigerode, which is similar to the St. Andreasberg vein system (Wilke 1952), formed at about 140 Ma (142 ± 2 Ma, K–Ar; 136 ± 3 and 138 ± 3 Ma, Ar–Ar; Hagedorn and Lippolt 1993). This age coincides with that obtained for the St. Andreasberg adularia (136 ± 3 Ma, K–Ar; Mertz et al. 1989), indicating that both ages are geologically meaningful. Consequently, a hematite-forming event could have taken place at ca. 135–140 Ma, which is temporally close to the Kupferschiefer metalliferous mineralisation at Sangerhausen, with which Late Jurassic hematite-rich (Rote Fäule) alteration is spatially associated (Symons et al. 2011). The temporal proximity of the above-mentioned ages and the specular hematite within the Roter Bär clausthalite could link the oxidising overprint at Roter Bär with the Rote Fäule at Sangerhausen. Such a temporal linkage, however, requires confirmation. Even if the Roter Bär hematite and the Rote Fäule hematite are not contemporaneous, their fluids could have had a common source—that is, fluids sourced from the sedimentary cover. In this regard, high-oxidation fluids from the Permo–Triassic red-bed sedimentary cover have been recorded in basement rocks immediately underneath the Variscan unconformity in the Spessart district (Fusswinkel et al. 2014).

Metallogenetic implications

The Roter Bär selenide occurrence has a Bi–Pb–Ag–(Au–Pd) metal association similar to post-Variscan, unconformity-related vein-type deposits, not only in central Europe, but also in the UK (Shepherd et al. 2005). Further similarities come from the oxic interface zone (equivalent to the Rote Fäule at Sangerhausen) immediately below the Kupferschiefer orebody in the Lubin mining district of Poland (Piestrzyński et al. 2002; Pieczonka and Piestrzyński 2005). This basin-wide oxic zone within the uppermost part of the Weissliegend sandstone is dominated by hydrothermal hematite and has gold contents up to the ppm range, and PGE contents in the 100-ppb range. The mineral association exhibits a great variety of selenides and arsenides of Cu, Pb, Bi, Pd, Ag, Au and Pd (Pieczonka and Piestrzyński 2005). Analogous metal and mineral assemblages, with clausthalite and klockmannite as the dominant selenides, have also been reported from the Rote Fäule zone at the Kupferschiefer deposit of Spremberg in Lower Lusatia, SE Germany (Kopp et al. 2012). Similar metal signatures, but lacking economic significance, have been observed in the cores of reduction spheroids in Permo–Triassic continental red beds of northern Switzerland (Hofmann 1990). The most common selenides in such reduction spheroids are clausthalite and bohdanowiczite. As pointed out by Hofmann (1990), during diagenesis of the red beds, metals were mobilised by brines at temperatures below 100 °C. The point to be made here is that oxidised brines led to the deposition of Bi selenides both in the Permian red beds and in the Variscan basement in the Harz (Roter Bär), as well as in other localities. This point implies that rocks of the Variscan basement and the Permo–Triassic sedimentary cover were affected by large-scale overprint by oxidised brines.

Conclusions

The Roter Bär mineral assemblage of hematite, clausthalite, bohdanowiczite and empirical $Bi_4Pb_3Ag_2Se_{10}$ precipitated at high oxidation. The deposit can be described as an oxidised variant of the five-element vein-style mineralisation. Comparison with natural occurrences and experimental work suggests that bohdanowiczite constrains the temperature of mineral formation to <120 °C. The selenide minerals at Roter Bär likely resulted from oxidised brines, the salinity of which was instrumental in transporting Bi and other metals. Bismuth, particularly as Bi-bearing selenides, seems to be typical of unconformity-related vein-type deposits in the Variscan orogen of central Europe. Identification of Bi–Se minerals can be used as evidence for metal transport by oxidised brines.

Acknowledgements This work was elaborated during the stay of A.R. Cabral in Germany, which was initially financed by the Deutsche Forschungsgemeinschaft (DFG, project CA 737/1-1), and later sponsored by VALE S.A. Our study was supported by the German BMBF cooperative project 'r4—Wirtschaftsstrategische Rohstoffe: ResErVar/Harz'. One anonymous reviewer and, in particular, Gregor Markl contributed to improve the manuscript; they are gratefully acknowledged.

References

Banaś M, Atkin D, Bowles JFW, Simpson PR (1979) Definitive data on bohdanowiczite, a new silver bismuth selenide. Mineral Mag 43:131–133

Baumann L, Werner CD (1968) Die Gangmineralisation des Harzes und ihre Analogien zum Erzgebirge und zu Thüringen. Ber deutsch Ges geol Wiss B 13:525–548

Baumann A, Grauert B, Mecklenburg S, Vinx R (1991) Isotopic age determinations of crystalline rocks of the Upper Harz Mountains, Germany. Geol Rundsch 80:669–690

Belendorff K (1997) Seltene Selenide und Selenite vom Trogtal bei Lautenthal, Harz. Mineralien-Welt 8(2):22–24

Boness M, Haack U, Feldmann KH (1990) Rb/Sr-Datierung der hydrothermalen Pb–Zn-Vererzung von Bad Grund (Harz), BRD. Chem Erde 50:1–25

Burisch M, Walter BF, Wälle M, Markl G (2016) Tracing fluid migration pathways in the root zone below unconformity-related hydrothermal veins: insights from trace element systematics of individual fluid inclusions. Chem Geol 429:44–50

Cabral AR, Koglin N, Brätz H (2012) Gold-bearing ferroselite ($FeSe_2$) from Trogtal, Harz, Germany, and significance of its Co/Ni ratio. J Geosci 58:265–272

Cabral AR, Ließmann W, Lehmann B (2015) Gold and palladium minerals (including empirical $PdCuBiSe_3$) from the former Roter Bär mine, St. Andreasberg, Harz Mountains, Germany: a result of low-temperature, oxidising fluid overprint. Mineral Petrol 109:649–657

Chakrabarti DJ, Laughlin DC (1981) The Cu–Se (copper–selenium) system. Bull Alloy Phase Diagr 2:305–315

Dill HG (1994) Facies variation and mineralization in central Europe from the Late Paleozoic through the Cenozoic. Econ Geol 89:268–287

Dolníček Z, Fojt B, Prochaska W, Kučera J, Sulovský P (2009) Origin of the Zálesí U–Ni–Co–As–Ag/Bi deposit, Bohemian Massif, Czech Republic: fluid inclusion and stable isotope constraints. Miner Deposita 44:81–97

Förster H-J (2005) Mineralogy of the U–Se-polymetallic deposit Niederschlema-Alberoda, Erzgebirge, Germany. IV. The continuous clausthalite–galena solid-solution series. Neu Jb Mineral Abh 181:125–134

Förster H-J, Cooper MA, Roberts AC, Stanley CJ, Criddle AJ, Hawthorne FC, Laflamme JHG, Tischendorf G (2003) Schlemaite, $(Cu,\square)_6(Pb, Bi)Se_4$, a new mineral species from Niederschlema-Alberoda, Erzgebirge, Germany: description and crystal structure. Can Miner 41:1433–1444

Förster H-J, Tischendorf G, Rhede D (2005) Mineralogy of the Niederschlema-Alberoda U–Se-polymetallic deposit, Erzgebirge, Germany. V. Watkinsonite, nevskite, bohdanowiczite and other bismuth minerals. Can Miner 43:899–908

Frebold G (1927) Beiträge zur Kenntnis der Erzlagerstätten des Harzes. II. Über einige Selenerze und ihre Paragenesen im Harz. Centralblatt Mineral Geol Paläont A 1927, pp 16–32

Fusswinkel T, Wagner T, Wälle M, Wenzel T, Heinrich CA, Markl G (2013) Fluid mixing forms basement-hosted Pb–Zn deposits: insight from metal and halogen geochemistry of individual fluid inclusions. Geology 41:679–682

Fusswinkel T, Wagner T, Wenzel T, Wälle M, Lorenz J (2014) Red bed and basement sourced fluids recorded in hydrothermal Mn–Fe–As veins, Sailauf (Germany): a LA–ICPMS fluid inclusion study. Chem Geol 363:22–39

Geilmann W, Rose H (1928) Ein neues Selenerzvorkommen bei St. Andreasberg im Harz. Neu Jb Mineral Geol Paläont Abh A 57:785–816

Goldschmidt VM, Hefter O (1933) Zur Geochemie des Selens. Nachrichten von der Gesellschaft der Wissenschaften zu Göttingen, Mathematisch-Physikalische Klasse, III/35–IV/36:245–252

Hagedorn B, Lippolt HJ (1993) Isotopic age constraints for epigenetic mineralizations in the Harz mountains (Germany) from K–Ar, $^{40}Ar/^{39}Ar$ and Rb–Sr data of authigenic K-feldspars. In: Möller P, Lüders V (eds) Formation of hydrothermal vein deposits—a case study of the Pb–Zn, barite and fluorite deposits of the Harz mountains. Monograph series on mineral deposits, vol 30. Borntraeger, Berlin-Stuttgart, pp 87–102

Heider J (2014) Die Selenidmineralisation der Grube Henriette. Aufschluss 65:216–226

Heider J, Siemroth J (2012) Die Selenidmineralisation im Grauwacke-Tagebau Rieder bei Gernrode, Harz. Aufschluss 63:213–223

Hofmann BA (1990) Reduction spheroids from northern Switzerland: mineralogy, geochemistry and genetic models. Chem Geol 81:55–81

Johan Z, Picot P, Ruhlmann F (1982) Evolution paragénétique de la minéralisation uranifère de Chaméane (Puy-de-Dôme), France: chaméanite, geffroyite et giraudite, trois séléniures nouveaux de Cu, Fe, Ag et As. Tschermaks Mineral Petr Mitt 29:151–167

Keutsch FN, Förster H-J, Stanley CJ, Rede D (2009) The discreditation of hastite, the orthorhombic dimorph of $CoSe_2$, and observations on trogtalite, cubic $CoSe_2$, from the type locality. Can Miner 47:969–976

Kissin SA (1992) Five-element (Ni–Co–As–Ag–Bi) veins. In: Sheahan PA, Cherry ME (eds) Ore deposit models. Geoscience Canada, Reprint series, vol 6, pp 87–99

Koch H-P (2008) Die Minerale der Grube “Frische Lutter” bei Bad Lauterberg, Harz. Aufschluss 59:65–76

Kopp JC, Spieth V, Bernhardt H-J (2012) Precious metals and selenides mineralisation in the copper-silver deposit Spremberg-Graustein, Niederlausitz, SE-Germany. Z Deutsch Gesell Geowiss 163:361–384

Kuschka E, Franzke HJ (1974) Zur Kenntnis der Hydrothermalite des Harzes. Z Geol Wiss 2:1417–1436

Ließmann W, Bock M (1993) Die Grube Roter Bär bei St. Andreasberg/Harz. Verlag Sven von Loga, Köln

Lüders V, Möller P (1992) Fluid evolution and ore deposition in the Harz Mountains (Germany). Eur J Mineral 4:1053–1068

Markl G (2015) Schwarzwald—Lagerstätten und Mineralien aus vier Jahrhunderten. Band I—Nordschwarzwald und Grube Clara. Bode, Edition Krüger-Stiftung, Lauenstein

Markl G, Burisch M, Neumann U (2016) Natural fracking and the genesis of five-element veins. Miner Deposita 51:703–712

Mertz DF, Lippolt HJ, Schnorrer-Köhler G (1989) Early Cretaceous mineralizing activity in the St. Andreasberg ore district (Southwest Harz, Federal Republic of Germany). Miner Deposita 24:9–13

Möller P, Morteani G, Hoefs J, Parekh PP (1979) The origin of the ore-bearing solution in the Pb–Zn veins of the western Harz, Germany, as deduced from rare-earth element and isotope distributions in calcites. Chem Geol 26:197–215

Oelsner OW (1958) Die erzgebirgischen Granite, ihre Vererzung und die Stellung der BiCoNi-Formation innerhalb dieser Vererzung. Geologie 7:682–701

Pieczonka J, Piestrzyński A (2005) New minerals from the red bed type precious metal deposit of the Lubin-Sieroszowice mining district, SW Poland. In: Mao JW, Bierlein FP (eds) Mineral deposit research: meeting the global challenge. Proceedings of the eighth Biennial SGA meeting in Beijing, China, 18–21 Aug 2005, vol 2. Springer, pp 1041–1044

Piestrzyński A, Pieczonka J, Głuszek A (2002) Redbed-type gold mineralisation, Kupferschiefer, south-west Poland. Miner Deposita 37:512–528

Pokrovsky GS, Borisova AY, Roux J, Hazemann J-L, Petdang A, Tella M, Testemale D (2006) Antimony speciation in saline hydrothermal fluids: a combined X-ray absorption fine structure spectroscopy and solubility study. Geochim Cosmochim Acta 70:4196–4214

Pokrovsky G, Gout R, Schoit J, Zotov A, Harrichoury J-C (1996) Thermodynamic properties and stoichiometry of As (III) hydroxide complexes at hydrothermal conditions. Geochim Cosmochim Acta 60:737–749

Pringle GJ, Thorpe RI (1980) Bohdanowiczite, junoite and laitakarite from the Kidd Creek mine, Timmins, Ontario. Can Miner 18:353–360

Ramdohr P, Schmitt M (1955) Vier neue natürliche Kobaltselenide vom Steinbruch Trogtal bei Lautenthal im Harz. Neu Jb Mineral Mh 6:133–142

Romer RL, Schneider J, Linnemann U (2010) Post-Variscan deformation and hydrothermal mineralization in Saxo-Thuringia and beyond: a geochronological review. In: Linnemann U, Romer RL (eds) Pre-Mesozoic geology of Saxo-Thuringia—from the Cadomian active margin to the Variscan Orogen. Schweizerbart, Stuttgart, pp 347–360

Schmidt Mumm A, Wolfgramm M (2004) Fluid systems and mineralization in the north German and Polish basin. Geofluids 4:315–328

Schneider J, Haack U, Stedingk K (2003) Rb–Sr dating of epithermal vein mineralization stages in the eastern Harz Mountains (Germany) by paleomixing lines. Geochim Cosmochim Acta 67:1803–1819

Schoell M (1970) K/Ar and Rb/Sr age determinations on minerals and total rocks of the Harz-Mountains/Germany. Eclogae Geol Helv 63:299

Sejkora J, Makovicky E, Topa D, Putz H, Zagler G, Plášil J (2011) Litochlebite, $Ag_2PbBi_4Se_8$, a new selenide mineral species from Zálesí, Czech Republic, description and crystal structure. Can Miner 49:639–650

Shepherd TJ, Bouch JE, Gunn AG, McKervey JA, Naden J, Scrivener RC, Styles MT, Large DE (2005) Permo–Triassic unconformity-related Au–Pd mineralisation, South Devon, UK: new insights and the European perspective. Miner Deposita 40:24–44

Simon G, Kesler SE, Essene EJ (1997) Phase relations among selenides, sulfides, tellurides, and oxides: II. Applications to selenide-bearing ore deposits. Econ Geol 92:468–484

Stanley CJ, Criddle AJ, Förster H-J, Roberts AC (2002) Tischendorfite, $Pd_8Hg_3Se_9$, a new mineral species from Tilkerode, Harz Mountains, Germany. Can Miner 40:739–745

Staude S, Werner W, Mordhorst T, Wemmer K, Jacob DE, Markl G (2012) Multi-stage Ag–Bi–Co–Ni–U and Cu–Bi vein mineralization at Wittichen, Schwarzwald, SW Germany: geological setting, ore mineralogy, and fluid evolution. Miner Deposita 47:251–276

Stedingk K, Stoppel D (1993) History of mining operations and economic importance of the Harz vein district. In: Möller P, Lüders V (eds) Formation of hydrothermal vein deposits—a case study of the Pb–Zn, barite and fluorite deposits of the Harz mountains. Monograph series on mineral deposits, vol 30. Borntraeger, Berlin-Stuttgart, pp 1–3

Stedingk K, Ließmann W, Bode R (2016) Harz. Bergbaugeschichte—Mineralienschätze—Fundorte. Bode, Edition Krüger-Stiftung, Lauenstein

Symons DTA, Kawasaki K, Walther S, Borg G (2011) Paleomagnetism of the Cu–Zn–Pb-bearing Kupferschiefer black shale (Upper Permian) at Sangerhausen, Germany. Miner Deposita 46:137–152

Thomas R, Tischendorf G (1987) Evolution of Variscan magmatic-metallogenetic processes in the Erzgebirge according to thermometric investigations. Z Geol Wiss 15:25–42

Tischendorf G (1959) Zur Genesis einiger Selenidvorkommen, insbesondere von Tilkerode im Harz. Freib Forschungshefte C 69:1–168

Tooth B, Etschmann B, Pokrovsky GS, Testemale D, Hazemann J-L, Grundler PV, Brugger JI (2013) Bismuth speciation in hydrothermal fluids: an X-ray absorption spectroscopy and solubility study. Geochim Cosmochim Acta 101:156–172

von Eynatten H, Voigt T, Meier A, Franzke H-J, Gaupp R (2008) Provenance of Cretaceous clastics in the Subhercynian Basin: constraints to exhumation of the Harz Mountains and timing of inversion tectonics in Central Europe. Int J Earth Sci (Geol Rundsch) 97:1315–1330

Wagner T, Okrusch M, Weyer S, Lorenz J, Lahaye Y, Taubald H, Schmitt RT (2010) The role of the Kupferschiefer in the formation of hydrothermal base metal mineralization in the Spessart ore district, Germany: insight from detailed sulfur isotope studies. Miner Deposita 45:217–239

Wallis E (1994) Erzparagenetische und mineralchemische Untersuchung der Selenide im Harz. Unpublished Diploma thesis, University of Hamburg, Hamburg, Germany

Walter BF, Burisch M, Markl G (2016) Long-term chemical evolution and modification of continental basement brines—a field study from the Schwarzwald, SW Germany. Geofluids 16:604–623

Wernick JH (1960) Constitution of the $AgSbS_2$–PbS, $AgBiS_2$–PbS, and $AgBiS_2$–$AgBiSe_2$ systems. Am Miner 45:591–598

Wilke A (1952) Die Erzgänge von St. Andreasberg im Rahmen des Mittelharz-Ganggebietes. Beih Geol Jb 7:1–228

Wood SA, Samson IM (1998) Solubility of ore minerals and complexation of ore metals in hydrothermal solutions. Rev Econ Geol 10:33–80

Wood SA, Crerar DA, Borcsik MP (1987) Solubility of the assemblage pyrite–pyrrhotite–magnetite–sphalerite–galena–gold–stibnite–bismuthinite–argentite–molybdenite in H_2O–NaCl–CO_2 solutions from 200 °C to 350 °C. Econ Geol 82:1864–1887

Xiong Y (2003) Predicted equilibrium constants for solid and aqueous selenium species to 300 °C: applications to selenium-rich mineral deposits. Ore Geol Rev 23:259–276

Zheng Y-F, Hoefs J (1993) Stable isotope geochemistry of hydrothermal mineralizations in the Harz mountains: II. Sulfur and oxygen isotopes of sulfides and sulfate and constraints on metallogenetic models. In: Möller P, Lüders V (eds) Formation of hydrothermal vein deposits—a case study of the Pb–Zn, barite and fluorite deposits of the Harz mountains. Monograph series on mineral deposits, vol 30. Borntraeger, Berlin-Stuttgart, pp 211–229